Picosecond excitation and selective intramolecular rates in supersonic molecular beams. I. SVL fluorescence spectra and lifetimes of anthracene and deuterated anthracenes

W. R. Lambert,[a] P. M. Felker,[b] and A. H. Zewail[c]
Arthur Amos Noyes Laboratory of Chemical Physics,[d] California Institute of Technology, Pasadena, California 91125

(Received 23 November 1983; accepted 8 December 1983)

Fluorescence spectra and decay rate results for jet-cooled anthracene and some deuterated anthracenes excited to single vibronic levels in their S_1 manifolds are presented. Consistent with our quantum beat results (see accompanying paper), fluorescence spectra exhibit the manifestations of negligible, then limited, and finally, extensive intramolecular vibrational energy redistribution (IVR), as the vibrational energy in S_1 is increased. The decay rate results indicate that the primary decay channel of the anthracenes for S_1 vibrational energies of 0 to 5600 cm^{-1} is a radiationless transition involving a small electronic energy gap. These decay rate results also display manifestations of negligible IVR at low energies and extensive IVR at higher energies. The energy at which the decay rates (time-resolved spectra) indicate extensive IVR is about 1800 cm^{-1}.

I. INTRODUCTION

Since our initial report[1] three years ago concerning the application of picosecond spectroscopy to jet-cooled anthracene, we have applied the technique to a number of other molecular systems. For instance, we have obtained results relevant to a number of problems including intramolecular quantum beats,[1-3] photoisomerization,[4] excited state proton transfer,[5] intramolecular exiplex formation,[6] and the photodissociation of hydrogen bonded complexes.[7] In a series of papers, of which this paper represents the first, we shall give full accounts of work pertaining to intramolecular reaction rates and quantum beats. Of initial concern will be the results of work on jet-cooled anthracene whose vibrational assignments are fully described in the previous paper.

In this paper we deal with single vibronic level (SVL) fluorescence spectra and lifetimes as a function of vibrational energy in the S_1 manifold of anthracene. In the paper[8] which immediately follows this one, we present a detailed study of quantum beats in anthracene excited to $S_1 + 1380$ cm^{-1}. Both papers focus on the problem of intramolecular vibrational energy redistribution (IVR) in large molecules. Since these first two papers involve extensive reference to anthracene spectroscopy, we have found it desirable to present them here in proximity to our paper[9] on the spectroscopy of jet-cooled anthracene. Paper III[10] of the series presents a study of the photochemistry of intramolecular exciplex formation in anthracene-$(CH_2)_3$-N,N-dimethylaniline. Finally, work for other papers[11] dealing with the dynamics of jet-cooled *t*-stilbene photoisomerization is forthcoming in this *Journal*.

This paper is outlined as follows: Section II briefly describes our experimental procedures, the details of which are presented in the accompanying paper. Section III gives the results of the time and energy-resolved fluorescence spectra. Also, in Sec. III we provide a discussion of these results in terms of IVR, and make the connection to the quantum beats results discussed in the following paper. Finally, some conclusions are given in Sec. IV.

II. EXPERIMENTAL PROCEDURES

A complete description of the experimental apparatus used to obtain the results reported in this paper is contained in the paper that follows.[8] Here, we present an outline of pertinent experimental methods.

H_{10}-, $9d_1$-, 9, $10d_2$- or d_{10}-anthracene at 150–180 °C was expanded with 30 psi of He or N_2 through an orifice with a diameter ($\equiv D$) of 100 or 150 μm. When N_2 was used as carrier gas, collisional effects were observed.[9] Therefore, most of the measurements reported herein were obtained using He expansions.

Excitation was provided by frequency doubling the output of a synchronously pumped, cavity-dumped picosecond dye laser using DCM as dye. The temporal width of the laser pulses was 15 ps. Either a two-plate birefringent filter, or a three-plate birefringent filter and fine tuning etalon were used as tuning elements, giving laser bandwidths of 2 Å and $\lesssim 0.5$ Å, respectively. Values of X/D (X being the laser-to-nozzle distance) were kept at > 30. Increasing this ratio beyond 30 did not result in any observable change in spectral or temporal results for He expansions.

Excitation to SVL's of h_{10}-anthracene was guided by reference to the normalized, high resolution excitation spectra of Ref. 9. For these measurements the laser wavelength (bandwidth $\lesssim 0.5$ Å) was calibrated using a calibrated monochromator. Errors in quoted absolute excitation frequencies are ± 5 cm^{-1}. The contribution of hot bands or van der Waals complexes at a given excitation energy could be as-

[a] Present address: Bell Laboratories, 600 Mountain Avenue, Murray Hill, New Jersey 07974.
[b] IBM Research Fellow.
[c] Camille and Henry Dreyfus Foundation Teacher–Scholar.
[d] Contribution No. 6948.

 0021-9606/84/172209-08$02.10

sessed by comparing the detected signal obtained using a He expansion with that obtained using a N_2 expansion.

For other measurements, excitation of anthracene and the deuterated species was accomplished using an excitation bandwidth of 2 Å and was guided by reference to the unnormalized, low resolution excitation spectra of Ref. 9. Errors in excitation energies for these data are laser-bandwidth limited. Specific experimental conditions will be noted with the data.

Fluorescence for the spectral measurements was collected using an $f/1$ lens and was then focused by another lens onto the slit of a microprocessor-controlled scanning monochromator. The monochromator was calibrated with a Fe–Ne lamp. Errors in relative frequencies are quoted to ± 5 cm^{-1}. The contribution of laser scatter to the resonance fluorescence band at a particular excitation energy could be assessed by observation of the time-resolved decay of this band: scatter appears as a fast component at $t = 0$. In the dispersed fluorescence spectra presented herein, the small scatter contribution has been subtracted from the resonance fluorescence. (This consideration was only important when resonance fluorescence was very weak.) No attempt was made to normalize spectra to laser power and spectra are not corrected for detector response.

Fluorescence for the temporal measurements was collected in two ways. In one way, the two-lens configuration used for the spectral measurements was used and the monochromator slits were opened to 3 mm (resolution$\equiv R = 50$ Å). This configuration was found to produce significant transit time effects for decays with lifetimes longer than ~ 10 ns. (The existence of transit time effects was deduced using several criteria: poor exponential fits, a dependence of fit lifetimes on carrier gas, and a dependence of lifetimes on the position of the collection lenses.) For more accurate lifetime measurements, the lens used to focus the fluorescence onto the monochromator slit was removed, and the $f/1$ collection lens was defocused. With the monochromator slits at 3 mm, this arrangement yielded a reduced signal compared to the two-lens system with the 3 mm slits, yet also eliminated transit time effects even for the longest decays measured (30 ns). It is pertinent to note that despite the poor fits of the lifetimes derived from measurements using the two-lens system these were fairly close in agreement to those that were obtained by using the one-lens configuration.

Fluorescence decays were fit to functions of the form $F(t) = Ae^{-t/\tau} + B$; where A, B, and τ are adjustable parameters. No attempt was made to deconvolute the data from the system response function since the lifetimes were long enough to neglect this factor. The quality of fits was judged by consideration of the reduced chi-squared parameter (χ_ν^2).[12] Typical values of this parameter for the fits of decays reported here are < 1.1. Lifetimes are quoted to $\pm 5\%$.

III. RESULTS AND DISCUSSION

A. Dispersed fluorescence spectra

We present in Figs. 1–4 SVL fluorescence spectra as a function of excitation energy for h_{10}-anthracene. The assignments of the particular SVL's that were excited may be found in Ref. 9. At a glance it is apparent that as the excitation energy increases, the spectra follow trends similar to those of the dispersed fluorescence spectra of other aromatics[13]: increased congestion and lack of sharp structure, decreased resonance fluorescence, spectral red shifts, and little further change in spectra above some excitation energy.

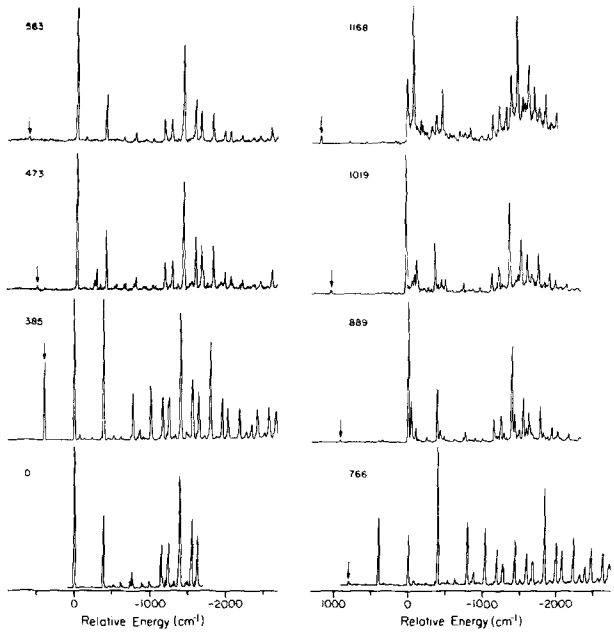

FIG. 1. Dispersed fluorescence spectra for some SVL's of anthracene having S_1 vibrational energies in the range of 0 to 1200 cm^{-1}. E_{vib} is given for each spectrum as is an arrow to indicate the spectral location of the exciting light. The abscissas represent energy scales relative to the 0_0^0 transition energy. Experimental conditions for all spectra: $X = 3$ mm, $D = 100$ μm, $T = 180$ °C, monochromator resolution ($\equiv R$) = 1.6 Å, carrier gas pressure ($\equiv P$) = 30 psi He, and laser bandwidth ($\equiv$BW)$\simeq$0.5 Å.

In the discussion of the spectral results, it will be convenient to divide the spectra into three groups corresponding to low, medium, and high excitation energy. Armed by the

TABLE I. Analysis of 12^1-level ($S_1 + 385$ cm^{-1}) fluorescence.

Shift from excitation energy (cm^{-1})	Intensity	Assignment
0	55	12_0^1
391	100	12_1^1
782	99	12_2^1
1175	33	12_3^1
1267	8	$12_0^1 7_1^0$
1408	40	$12_0^1 6_1^0$
1567	30	$12_4^1, 12_0^1 4_1^0, 12_1^1 8_1^0$
1654	30	$12_1^1 7_1^0, 12_0^1 \bar{3}_1^0$
1799	90	$12_1^1 6_1^0$
1956	43	$12_1^1 4_1^0$
2036	35	$12_1^1 \bar{3}_1^0$
2194	70	$12_2^1 6_1^0$
2350	30	$12_2^1 4_1^0$
2423	20	$12_2^1 \bar{3}_1^0$

TABLE II. Analysis of 11^1-level ($S_1 + 583\ cm^{-1}$) fluorescence.

Shift from excitation energy (cm^{-1})	Intensity	Assignment
0	<5	11_0^1
627	100	11_1^1
1020	38	$11_1^1 12_1^0$
1792	20	$11_1^1 8_1^0$
1887	20	$11_1^1 7_1^0$
2035	75	$11_1^1 6_1^0$
2192	33	$11_1^1 4_1^0$
2267	25	$11_1^1 \bar{3}_1^0$
2427	24	$11_1^1 12_1^0 6_1^0$

results of the accompanying paper, the features of the spectra will be explained in terms of coupling between S_1 vibrational levels.

Although we do not present spectra for the deuterated species, such measurements have been made.[14] The results are very similar to the h_{10}-anthracene results.

1. Low energy spectra: 0 to 1200 cm^{-1}

From Fig. 1 it is apparent that the SVL fluorescence spectra corresponding to excitation energies from 0 to 1200 cm^{-1} consist of discrete bands relatively free from congestion. These features immediately suggest that in this energy regime the coupling of optically prepared vibrational levels to other levels in the S_1 manifold is minimal. Closer analysis of the spectra bears this interpretation out. For example, in Tables I and II the spectra (see Fig. 1) resulting from the excitation of the 12^1 ($E_{vib} = 385\ cm^{-1}$) and 11^1 ($E_{vib} = 583\ cm^{-1}$) SVL's are respectively analyzed. All of the major features in both spectra may be assigned as transitions arising from the optically prepared level (i.e., 12^1 or 11^1). For both levels this indicates the absence of extensive vibrational mixing. In this regard, it is interesting to note that the 11^1 spectrum shows very little resonance fluorescence in contrast to the 12^1 spectrum. This behavior reflects the fact that the "11" mode is much less optically active than the "12" mode[9] (by optically active we mean that in a transition the vibrational quantum number need not equal zero), and has little or nothing to do with vibrational mixing involving the 11^1 level.

Several spectra at the high energy end of the 0 to 1200 cm^{-1} range exhibit bands which are not readily assignable in terms of transitions from the optically prepared level. For example, in the $\bar{9}^1$ ($S_1 + 889\ cm^{-1}$) spectrum, there is a band at a shift of 957 cm^{-1} with about one-third the intensity of the $\bar{9}_1^1$ (917 cm^{-1}) band. It is possible that this band results from the coupling of the $\bar{9}^1$ level with another vibrational level. Similar bands occur in the $S_1 + 1019$ and $S_1 + 1165$ cm^{-1} spectra. These spectra exemplify the fact that the division of spectral results into three categories is somewhat artificial. It is important to point out that within a given energy category complete generalizations with regard to vibrational coupling may not be possible and that differences in this coupling may occur within a category.

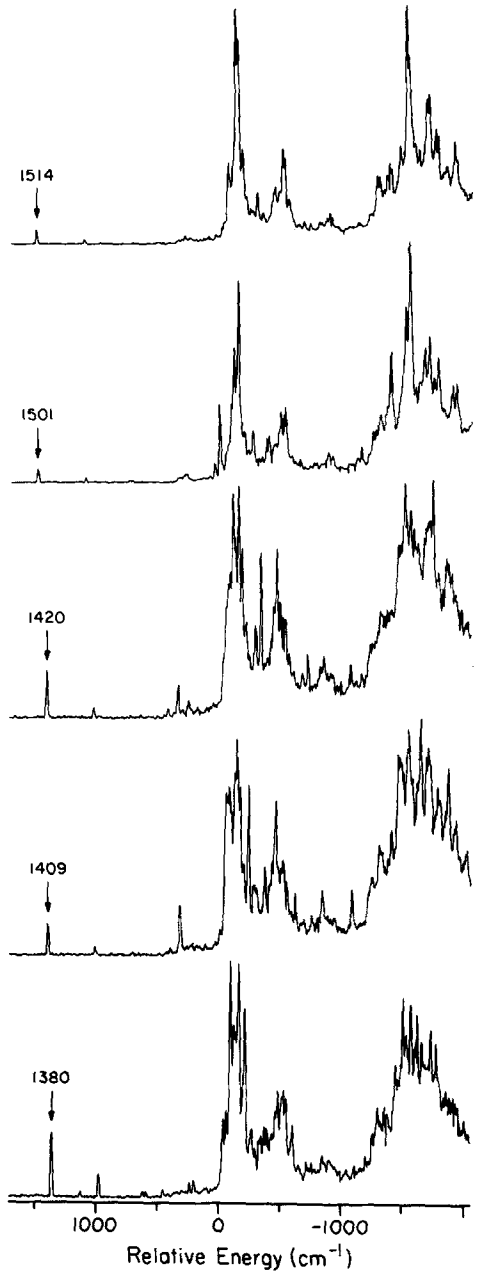

FIG. 2. Dispersed fluorescence spectra for some SVL's of anthracene having energies in the range of 1300–1600 cm^{-1}. The arrows, numbers, and abscissa all have the same meanings as in Fig. 1. Experimental conditions are the same as for Fig. 1.

2. Intermediate energy spectra: 1300–1600 cm^{-1}

The SVL spectra of Fig. 2 corresponding to S_1 vibrational energies from ~1300 to 1600 cm^{-1} are characterized primarily by the congested, though resolvable, structure that occurs both near and to the red of the 0_0^0 transition energy (27 695 cm^{-1}, 3610.8 Å).[9] In addition, several of the spectra exhibit significantly intense resonance fluorescence bands as well as bands in the uncongested region to the blue of the 0_0^0 energy. It is convenient in analyzing the features of the spectra in this energy region to consider one spectrum in particular, which contains many of the features common to all the spectra. Thus, presented in Table III is a summary of band positions, intensities, and assignments for the 6^1 (1380 cm^{-1}) SVL spectrum.

TABLE III. Analysis of 6^1-level ($S_1 + 1380\ cm^{-1}$) fluorescence (see Figs. 2 and 3).[a]

Shift from excitation energy (cm^{-1})	Intensity	Assignment
0	28	6_0^1
233	4	$6^1 \rightarrow S_0$ + lowest energy b_{3g}
389	11	$6_0^1 12_1^0$
624	3	$6_0^1 11_1^0$
750	4	$6_0^1 10_1^0$
778	4	$6_0^1 12_2^0$
912	5	$6_0^1 \bar{9}_1^0$
1125	8	?
1162	9	$6_0^1 8_1^0$
1244	5	?
1261	5	$6_0^1 7_1^0$
1403	34	6_1^1
1429	38	?
1460	100	?
1470	50	?
1490	75	$6_0^1 5_1^0$?
1505	60	?
1514	60	(1125 + 390)
1528	62	?
1534	65	?
1564	50	$6_0^1 4_1^0$
1581	80	?, $6_0^1 \bar{4}_1^0$

[a] For ground state intervals of anthracene see Ref. 9.

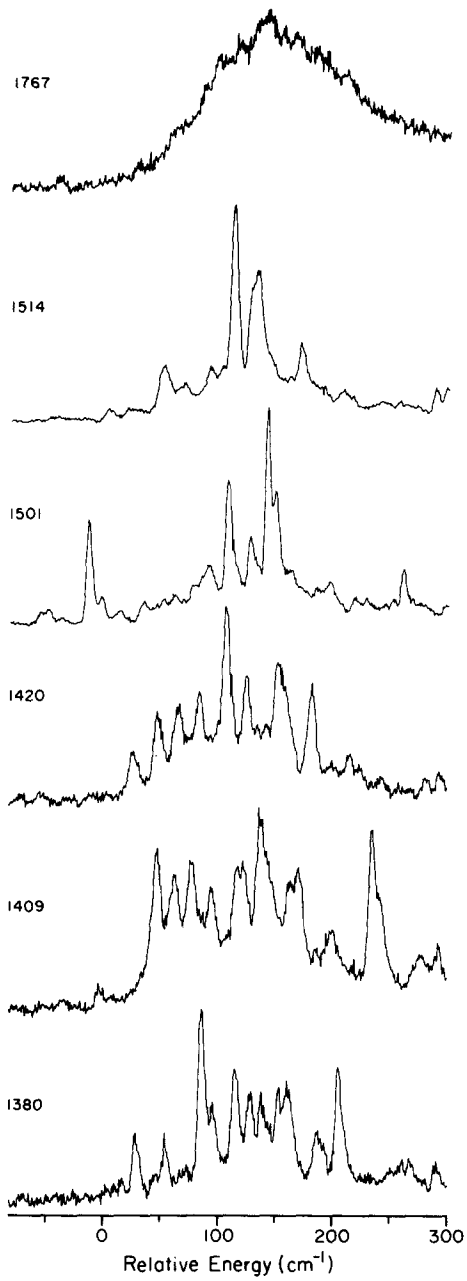

FIG. 3. High resolution spectra for medium energy range SVL's. The numbers again represent the S_1 vibrational energy and the abscissa is relative to the 0_0^0 transition energy. For all spectra $X = 3$ mm, $D = 100\ \mu$m, $T = 180$ °C, $P = 30$ psi He, BW$\simeq$0.5 Å. For the 1380 and 1501 cm^{-1} spectra, $R = 0.5$ Å. For all others, $R = 0.7$ Å. The uppermost spectrum is included to illustrate the broadening that occurs at higher excitation energies.

The 6^1 SVL involves one quantum of the strongly optically active $a_g(6)$ mode (ground state value of 1408 cm^{-1}).[9] In the absence of extensive vibrational mixing between this level and other vibrational levels, one would only expect significantly intense fluorescence bands at those energies corresponding to 6_n^1 transitions and combination bands of the form[15] $6_n^1\ \{A\}_{\{m\}}^{\{0\}}$, where $\{A\}$ is some set of optically active modes. Reference to Table III shows that such bands are indeed observed in the 6^1 spectrum. However, the intensities of these bands are no greater, and in most cases smaller than the intensities of those bands in the congested region of the spectrum which are not readily assignable in terms of fundamentals, overtones, or combination bands of optically active ground state modes.

The features of the 6^1 spectrum can be explained in terms of intermediate case coupling between vibrational levels. In this scheme, the 6^1 optically active state is coupled to a small set of discrete, near resonant vibrational levels of the form $\{A'\}^{\{m'\}}\{B'\}^{\{l'\}}$, where $\{A'\}$ is some set of optically active modes and $\{B'\}$ some set of optically inactive modes. This coupling results in a set of eigenstates having contributions from the 6^1 level and the $\{A'\}^{\{m'\}}\{B'\}^{\{l'\}}$-type levels. Upon excitation of this set of eigenstates, not only will fluorescence bands of the type $6_n^1\{A\}_{\{m\}}^{\{0\}}$ be observed but also bands of the form $\{A'\}_{\{m'\}}^{\{m'\}}\{B'\}_{\{l'\}}^{\{l'\}}$. The unassignable bands in the 6^1 spectrum can be attributed to this latter kind of band. The prevalence of these bands near and to the red of the 0_0^0 transition energy reflects the fact that the number of strongly optically active modes is much less than the number of inactive ones. Because of this, most of the coupled $\{A'\}^{\{m'\}}\{B'\}^{\{l'\}}$-type levels have $\{m'\} = \{0\}$. The fluorescence contribution arising from one of these levels $\{A'\}_{\{m'\}}^{\{0\}}\{B'\}_{\{l'\}}^{\{l'\}}$ is a 0^0-like spectrum with an origin $\{B'\}_{\{l'\}}^{\{l'\}}$ near the 0_0^0 transition energy.

The number of coupled levels is indicated by two features of the 6^1 fluorescence spectrum; the degree of congestion and the amount of $6_n^1\{A\}_{\{m\}}^{\{0\}}$ fluorescence. The existence in the 6^1 spectrum of structure resolvable by using several cm^{-1} resolution, and the existence of $6_n^1\{A\}_{\{m\}}^{\{0\}}$ bands of significant intensity, indicate that the number of coupled levels is small, i.e., on the order of ten or less. It is

pertinent to note that evidence[9,16] exists indicating that the ground state 6_1 level also is coupled to a sparse manifold of vibrational levels. Vibrational coupling in the ground state may also be expected to contribute to congestion in the spectrum. Such congestion might complicate the interpretation of spectra in terms of IVR.

Features of other SVL spectra in this energy region support the picture of optically prepared states coupled to a coarse manifold of levels. In particular, note the spectra of Fig. 3 which are higher resolution portions of some of the spectra in Fig. 2. All of the spectra, though congested, have resolvable vibronic bands in the spectral region near the 0_0^0 transition energy. But, the distribution of emission bands strongly differs from spectrum to spectrum. This variation reflects the discrete nature of the coupled $\{A'\}^{\{m'\}}\{B'\}^{\{l'\}}$ levels and contrasts with a lack of similar variation in higher energy spectra. It is interesting to note that density of states calculations, using direct counting of states, and the vibrational frequencies of Refs. 17 and 18, yield vibrational densities of states of all types of symmetry of ~20–60 cm in the 1300–1600 cm^{-1} region of the S_1 manifold. Given symmetry selection rules for coupling between vibrational levels and the linewidth of the states involved, these values for $\rho(E_{vib})$ are consistent with an intermediate case coupling scheme: the average separation between interacting levels (600 MHz or greater) is much larger than the intrinsic width (~20 MHz).

This picture is confirmed by time-resolved results for the excitation of several bands in the 1300–1600 cm^{-1} spectral region which display manifestations (quantum beats) typical of coupling to a relatively sparse manifold.[1,3] Some of these results shall be detailed in the following paper.[8]

3. High energy spectra: 1600 cm^{-1} and up

Figure 4 presents spectra corresponding to excitation of S_1 levels having vibrational energies greater than 1600 cm^{-1}. Similar results have also been obtained for E_{vib} up to 5600 cm^{-1}. The spectra, which are very similar to bulb results,[19] are characterized by the absence (or very little) of resonance fluorescence, and by spectral envelopes which both change very little as the excitation energy changes and appear like extensively broadened, red-shifted 0^0-level fluorescence.

The general features of a typical spectrum in this excitation energy regime can be explained in terms of an optically active zero-order level $\{A\}^{\{m\}}$, coupled to a large number of other levels of the type $\{A'\}^{\{m'\}}\{B'\}^{\{l'\}}$ ($\{A'\}$ and $\{B'\}$ having the same definitions as before). The 0^0-like shape of the observed spectral envelope is a consequence of the fact that most of the coupled levels have $\{m'\} = \{0\}$ (see above) and that each such level gives rise to a fluorescence contribution consisting of a 0^0-like spectrum with the $\{B'\}^{\{l'\}}_{\{l'\}}$ band serving as an origin. (Note that some levels with $\{m'\} \neq 0$ do contribute weakly to observed fluorescence. The most significant contributions of this sort come from levels of the form $12^1\{B'\}^{\{l'\}}$, which, e.g., give rise to the small hump to the blue of the 0^0 energy in the spectra of Fig. 4.) The overall red shift of the typical spectrum relative to the 0^0 spectrum arises

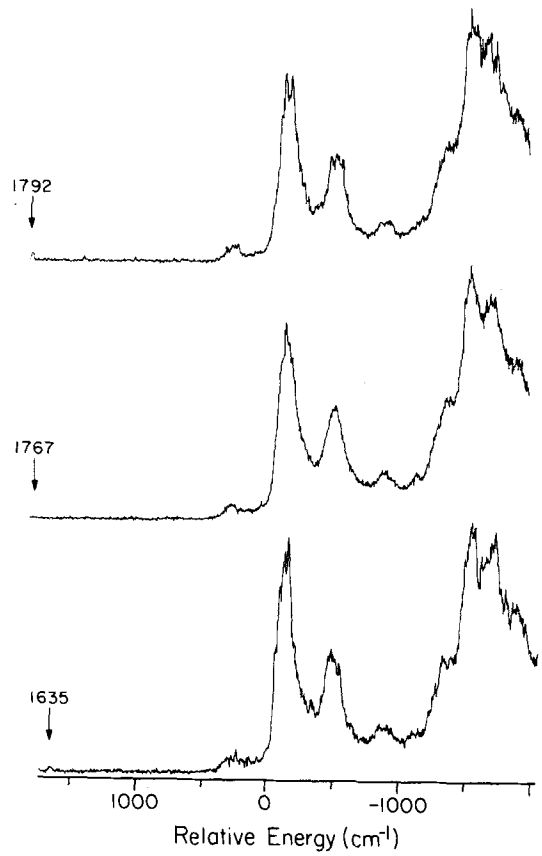

FIG. 4. High energy SVL fluorescence spectra. All notations and experimental conditions are the same as for Figs. 1 and 2.

because most vibrational modes in anthracene have higher frequencies in S_0 than in S_1. On the average, therefore, the transition frequencies of the $\{B'\}^{\{l'\}}_{\{l'\}}$-type bands are less than that of the 0^0 band. The broadness of the spectral features is due to the large number of zero-order levels contributing to the fluorescence and also to the dispersion in the transition energies of the $\{B'\}^{\{l'\}}_{\{l'\}}$-type bands. The lack of resonance fluorescence may be attributed to the extensive dilution of the $\{A\}^{\{m\}}$ zero-order state by coupling to other levels. Finally, both the large number of coupled levels, and the dominance, in the coupling, of levels which give rise to 0^0-like fluorescence contribute to the relatively unchanging nature of the spectra in this energy regime.

B. Fluorescence decay rate measurements

Figures 5 and 6 present the results of SVL fluorescence decay measurements made on the anthracene species. In addition, contained in Table IV are the lifetimes of the species at selected excitation energies. The lifetimes for various low energy excitation bands of h_{10}-anthracene can be compared with literature values: our values of 21.5,[1] 27.5, and 15.3 ns for the 0, 232, and 385 cm^{-1} bands are reasonably close to the values taken from Ref. 20: 24, 30.5, and 17 ns. The reason for the systematic small difference in results is probably due to the convolution procedure used in Ref. 20. The trend of the results for the protonated species also is consistent with results[21] of quantum yield measurements made as a function of excitation energy and with recent electronic state lifetime measurements.[21(b),21(c)] As is evident from the figure cap-

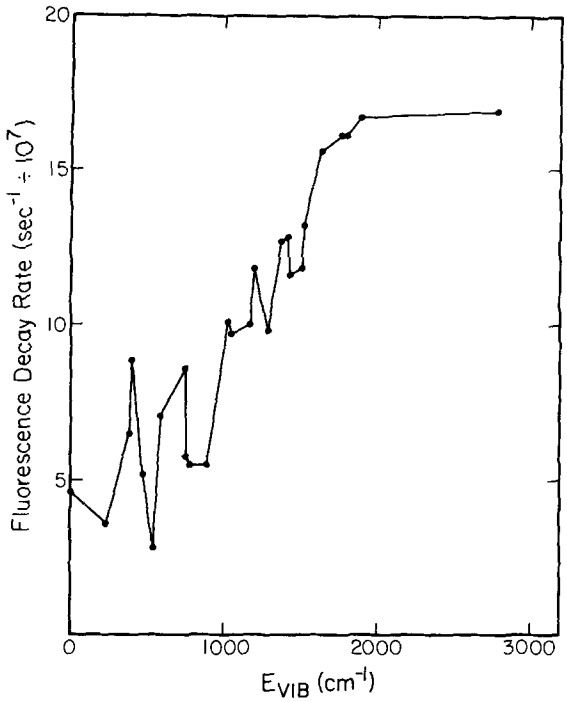

FIG. 5. h_{10}-anthracene fluorescence decay rate as a function of S_1 vibrational energy. For all data points $X = 3$ mm, $D = 100\,\mu$m, $T = 180$ °C, $P = 30$ psi He, BW≃0.5 Å, and detection wavelength = 3800 Å with $R = 50$ Å. The lines connecting points are meant only as guides to the eye.

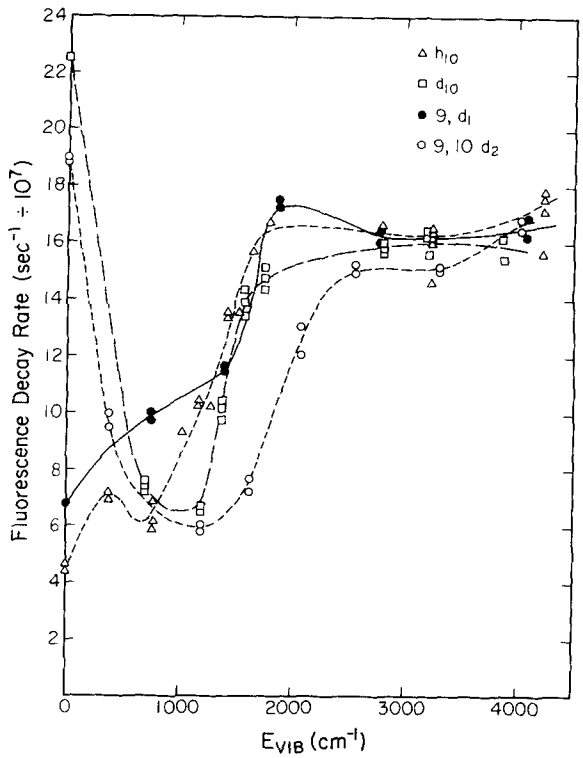

FIG. 6. Fluorescence decay rates of all the anthracene species as a function of S_1 vibrational energy. $X = 5$ mm, $D = 150\,\mu$m, $P = 45$ psi N_2, $T = 180$ °C, BW = 2 Å, and detection wavelength ≃3800 Å. The lines connecting points are meant only as guides to the eye.

tions, the sets of data for Figs. 5 and 6 were obtained using quite different experimental conditions. Despite this, there is agreement between the results in the two figures.

Various points may be noted regarding the decay results. Firstly, it is clear that all of the curves in Figs. 5 and 6 saturate at high energies. For h_{10}-anthracene the fluorescence lifetimes stay relatively constant from 1700 (6.2 ns) to 5600 cm^{-1} (5.7 ns—not shown in the figures). The lifetime values at these high energies are very close to lifetimes measured for anthracene in a bulb.[22] Secondly, there are marked fluctuations in decay rate at low excess energies, which do not appear at high energies. Finally, there is no pronounced deuterium isotope effect except at low excess energies, where the effect is actually the opposite of the "normal" effect,[23] and is very dramatic!

Consideration of the decay trends noted above can lead to conclusions regarding the dominant deactivation process contributing to S_1 decay in cold, isolated anthracenes.[24] In particular, the results indicate that this decay channel involves the interaction of S_1 levels with the levels of a close-lying electronic state (i.e., one within several thousand wave numbers of S_1). Results of theoretical calculations[25,26] for large energy gap processes in large molecules predict an approximately exponential increase in the radiationless rates of large molecules as the energy of the molecule increases. This is certainly not in agreement with the lifetime *saturation* observed for anthracene. On the other hand, other theoretical work[26] has predicted virtually no variation of decay rate with molecular energy for naphthalene S_1–T_n intersystem crossing (ISC) involving a small electronic state energy gap (1400 cm^{-1}). Secondly, the lack of the well known deuterium isotope effect at the higher excitation energies is indicative of a process involving a small energy gap.[24] The presence of an actual inverse isotope effect on lifetimes in the low energy regime is most probably due to the involvement of nearby triplet states in the nonradiative decay. Our results on the lifetime and inverse isotope effect are in agreement with the results of quantum yield obtained by Jortner *et al.* and lifetimes by Lim *et al.*[21] Finally, experiments[27] on anthracene in solution indicate that ISC from S_1 to higher-lying triplet states is an important fluorescence decay channel. Pariser's calculations[28] place several triplet states in the vicinity of S_1.

Knowledge of the energy gap pertinent to the decay process of S_1 anthracene is useful information in attempting to link fluorescence lifetime behavior to IVR. Taking this gap in anthracene to be small, using the theoretical results of Fischer, Schlag, and Schneider (FSS)[26] and our experimental results, it is possible to make qualitative statements regarding the extent of IVR as a function of S_1 vibrational energy. As mentioned above, FSS have calculated rate vs energy curves that are essentially flat for small energy gap processes in naphthalene. A major assumption underlying these calcu-

TABLE IV. Representative lifetimes (ns) of anthracene species at zero and high S_1 vibrational energy.[a]

S_1 vibrational energy (cm^{-1})	h_{10}	$9d_1$	$9,10d_2$	d_{10}
0	21.5	14.8	5.1	4.4
~4000	5.7	6	6	6.2

[a] For excess energy dependence of lifetimes see Figs. 5 and 6.

lations is that IVR occurs on a time scale that is very short compared to the inverse rate of the decay process. Assuming the validity of extending their results to anthracene, it is plausible to attribute the saturation effect in the high energy portions of our rate vs E curves to a situation wherein radiationless decay occurs after rapid and extensive IVR. However, this interpretation is only valid if a similar saturation effect is not expected in the limit of no IVR. In fact, Franck–Condon considerations[29] indicate that, in general, increased vibrational excitation results in increased radiationless rates irrespective of the energy gap, when IVR is not occurring. With this in mind the results of Figs. 5 and 6 are understandable in terms of two energy regimes. In the region below $\sim 1800\ \mathrm{cm}^{-1}$, IVR is limited or absent on the time scale of the S_1 lifetime. The result is a general increase in radiationless rate with energy. In addition, the curve of rate vs E is not monotonic owing to the Franck–Condon factor changes[29] which occur with changes in the nature of the vibrational level that is excited. Above $1800\ \mathrm{cm}^{-1}$ extensive IVR occurs and results in the lifetime saturation predicted by FSS for small energy gaps. Note that no significant fluctuations of rate vs energy occur in this energy regime; this being consistent with a large distribution of emitting vibrational levels. This picture we have given concerning the link between IVR and lifetime trends in anthracene is further supported by correlation of the lifetime results with SVL fluorescence spectra. In particular, it is notable that lifetime saturation occurs in roughly the same excitation energy region in which the dispersed fluorescence spectra indicate extensive broadening and vibrational mixing.

It is appropriate to mention that the interpretation of rate vs energy curves in terms of IVR is not without many difficulties. For instance, we have assumed the existence of one dominant decay channel involving a small electronic energy gap. Given the number of electronic states in anthracene predicted to be near S_1,[28] this assumption may not be valid. It is unclear how the involvement of more than one accepting electronic state would modify the argument put forth by us above. Also, the possibility of changes in molecular geometry with increasing energy has not been taken into account here. Such changes have been suggested to be involved in lifetime saturation effects in other molecules.[25(d)] Finally, the FSS theory has been criticized in that it apparently introduces a significant spread in the total molecular vibrational energy.[25(c)] Again, it is not clear just how this affects the interpretation. Despite these difficulties, our experimental results showing a correlation between lifetime saturation and spectral broadening, and showing lifetime fluctuations in the low energy region compared to no such fluctuations at high energies, are telling pieces of information pointing to the usefulness of fluorescence lifetime measurements as a sensor of IVR in anthracene.

As a final point regarding the decay data of h_{10}-anthracene, it is interesting to note the long lifetimes, 27.5 and 35.2 ns, of the SVL's at $S_1 + 232$ and $S_1 + 541\ \mathrm{cm}^{-1}$, respectively. Spectral evidence[9] suggests that both of these levels involve the excitation of a greatly perturbed S_1 "$\overline{11}$" mode. The lifetime data further reinforce the interpretation that the two levels are closely associated. Conversely, if one accepts the assignment[9] of the levels as $\overline{11}^1$ and $\overline{11}^2$, then the lifetimes suggest that excitation of the "$\overline{11}$" mode acts as an inhibitor to the dominant radiationless decay process of S_1 anthracene.

IV. CONCLUSION

We have presented SVL fluorescence spectra and lifetimes for anthracene and some deuterated derivatives. The results have been discussed primarily in terms of IVR processes. The dispersed fluorescence spectra indicate increased vibrational mixing with the S_1 manifold as the vibrational energy increases. Of particular interest are spectra obtained for excitation to $S_1 + 1300$ to $1600\ \mathrm{cm}^{-1}$ since they represent manifestations of the transition from negligible to extensive IVR. The existence of restricted IVR is experimentally demonstrated by the quantum beat results (see Refs. 3 and 8) on anthracene. Our spectra presented here are consistent with the work of Tramer's group on perylene, and Amirav *et al.*[30] on tetracene. Trends in the lifetime results are closely correlated with SVL spectral trends. In particular, a saturation of the rate vs E curves occurs at $\sim 1800\ \mathrm{cm}^{-1}$. This corresponds to an energy at which extensive IVR is indicated by SVL spectra. Theoretical results indicate that the lifetime saturation can be accounted for by assuming a small energy gap decay process and extensive IVR. It is evident that SVL fluorescence spectra and lifetimes taken together can be qualitatively used as probes of IVR in large molecules. More direct measurements[3] of IVR processes will be dealt with in the following paper.

ACKNOWLEDGMENTS

It is a pleasure to acknowledge the support of this work by the National Science Foundation. We wish to thank Professor Joshua Jortner for informing us of their recent work on quantum yield measurements.

[1] Wm. R. Lambert, P. M. Felker, and A. H. Zewail, J. Chem. Phys. **75**, 5958 (1981).
[2] P. M. Felker, Wm. R. Lambert, and A. H. Zewail, Chem. Phys. Lett. **89**, 309 (1982).
[3] P. M. Felker and A. H. Zewail, Chem. Phys. Lett. **102**, 113 (1983).
[4] J. A. Syage, W. R. Lambert, P. M. Felker, A. H. Zewail, and R. M. Hochstrasser, Chem. Phys. Lett. **88**, 266 (1982).
[5] P. M. Felker, Wm. R. Lambert, and A. H. Zewail, J. Chem. Phys. **77**, 1603 (1982).
[6] P. M. Felker, J. A. Syage, Wm. R. Lambert, and A. H. Zewail, Chem. Phys. Lett. **92**, 1 (1982).
[7] P. M. Felker and A. H. Zewail, Chem. Phys. Lett. **94**, 448, 454 (1983); P. M. Felker and A. H. Zewail, J. Chem. Phys. **78**, 5266 (1983).
[8] W. R. Lambert, P. M. Felker, and A. H. Zewail, J. Chem. Phys. **81**, 2217 (1984).
[9] W. R. Lambert, P. M. Felker, J. A. Syage, and A. H. Zewail, J. Chem. Phys. **81**, 2195 (1984).
[10] J. A. Syage, P. M. Felker, and A. H. Zewail, J. Chem. Phys. **81**, 2233 (1984).
[11] J. A. Syage, P. M. Felker, and A. H. Zewail, J. Chem. Phys. (to be published).
[12] P. R. Bevington, *Data Reduction and Error Analysis for the Physical Sciences* (McGraw–Hill, New York, 1969).
[13] For example: (a) P. S. H. Fitch, L. Wharton, and D. Levy, J. Chem. Phys. **70**, 2018 (1979); (b) S. M. Beck, J. B. Hopkins, D. E. Powers, and R. E. Smalley, *ibid.* **74**, 43 (1981); (c) A. Amirav, U. Even, and J. Jortner, *ibid.*

74, 3745 (1981); (d) C. Bouzou, C. Jouvet, J. B. Leblond, Ph. Millie, A. Tramer, and M. Sulkes, Chem. Phys. Lett. **97**, 161 (1983).
[14]W. R. Lambert, Ph.D. thesis, California Institute of Technology, 1982.
[15]The notation for vibrational levels and for S_1–S_0 transitions is the same as that used in the Ref. 9. In addition, whenever brackets—{ }—appear, a set is intended. Thus $\{A\}^{\{m\}}$ implies an excited state vibrational level involving A-type modes characterized by the set of quantum number $\{m\}$ (i.e., $A'^{m}A''^{m}A'''^{m}\ldots$).
[16]T. P. Carter and G. D. Gillespie, J. Phys. Chem. **86**, 2691 (1982).
[17]B. N. Cyvin and S. J. Cyvin, J. Phys. Chem. **73**, 1430 (1969).
[18]D. J. Evans and D. B. Scully, Spectrochim. Acta. **20**, 891 (1964).
[19]For example, R. St. Dygdala and K. Stefanski, Chem. Phys. **53**, 51 (1980).
[20]T. R. Hays, W. Henke, H. L. Selzle, and E. W. Schlag, Chem. Phys. Lett. **77**, 19 (1981).
[21](a) A. Amirav and J. Jortner, Chem. Phys. Lett. **94**, 545 (1983); (b) A. Amirav, M. Sonnenschein, and J. Jortner (to be published); (c) E. Lim (to be published).
[22]W. R. Ware and P. T. Cunningham, J. Chem. Phys. **43**, 3826 (1965).
[23]See, for example, (a) G. W. Robinson and R. P. Frosch, J. Chem. Phys. **38**, 1187 (1963); (b) W. Siebrand, in *The Triplet State*, edited by A. Zahlan (Cambridge University, London, 1967); (c) E. C. Lim and H. Bhattacharjee, Chem. Phys. Lett. **9**, 249 (1971).
[24]Note that we assume that the variations in measured lifetimes may be attributed solely to variations in nonradiative decay rates. This is consistent with the quantum yield data of Ref. 21(a).
[25](a) S. Fischer, Chem. Phys. Lett. **4**, 333 (1969); (b) S. Fischer and E. W. Schlag, *ibid* **4**, 393 (1969); (c) K. F. Freed, Top. Appl. Phys. **15**, 24 (1976); (d) T. G. Dietz, M. A. Duncan, A. C. Piui, and R. E. Smalley, J. Phys. Chem. **86**, 4026 (1982).
[26]S. Fischer, E. W. Schlag, and S. Schneider, Chem. Phys. Lett. **11**, 583 (1971).
[27]U. Laor, J. C. Hsieh, and P. K. Ludwig, Chem. Phys. Lett. **22**, 150 (1973).
[28]R. Pariser, J. Chem. Phys. **24**, 250 (1956).
[29]W. Siebrand, J. Chem. Phys. **54**, 363 (1971).
[30]A. Amirav, U. Even, and J. Jortner, J. Chem. Phys. **75**, 3770 (1981).